Journal of Alloys and Compounds 701 (2017) 574–580

Contents lists available at ScienceDirect

Journal of Alloys and Compounds

journal homepage: http://www.elsevier.com/locate/jalcom

Topaz synthesis using Al_2O_3, $Al(OH)_3$ or $Al_2Si_2O_5(OH)_4$ and color centers promoting its radioluminescence response

E. Trujillo-Vázquez [a], M.I. Pech-Canul [a, *], J. Marcazzó [b]

[a] Centro de Investigación y de Estudios Avanzados del Instituto Politécnico Nacional, Unidad Saltillo. Av. Industria Metalúrgica No. 1062, Parque Industrial Saltillo-Ramos Arizpe, Ramos Arizpe, Coahuila, 25900, Mexico
[b] Instituto de Física Arroyo Seco (UNCPBA) and CIFICEN (UNCPBA – CICPBA – CONICET), Pinto 399, 7000 Tandil, Argentina

ARTICLE INFO

Article history:
Received 9 November 2016
Received in revised form
8 January 2017
Accepted 16 January 2017
Available online 18 January 2017

Keywords:
CVD-topaz
Radioluminescence
Irradiation
^{90}Sr beta-source
Alternative reactants
$(H_3O_4)^0$ color centers

ABSTRACT

A first study on the radioluminescence (RL) response of topaz synthesized is reported. Using three alternative and different compact reactants separately, i. e., aluminum oxide, aluminum hydroxide and kaolinite, synthesis tests by chemical vapor deposition (CVD) were conducted varying systematically processing temperature and time, incidence angle, and atmosphere. Results show the feasibility to form topaz using the three types of reactants, in varying amounts of 60%, 100% and 47%, respectively. Synthesized topaz exhibits a variety of morphologies: fibers and rectangular bars using Al_2O_3, cross needle shape compacts using $Al(OH)_3$ and needle-shape phases using $Al_2Si_2O_5(OH)_4$. Irradiation with ^{90}Sr beta-source revealed that only samples prepared using aluminum hydroxide exhibit RL response. The emission band centered at 390 nm of thermally untreated samples and the lack of RL emission of samples treated thermally at 500 °C confirm that the RL response is due to the $(H_3O_4)^0$ color centers. The RL response showing the highest RL intensity at 390 nm is promoted by processing at 700 °C for 90 min, used for sample H3. A set of reaction pathways for topaz formation using the three alternative compact reactants is proposed.

1. Introduction

Radioluminescence (RL) is the phenomenon by which a material produces light by bombardment with ionizing radiation. Some minerals like topaz [1], which pertains to the group of alumino-silicates, exhibit this property. Topaz is one of the main fluorine bearing minerals that comprises a solid solution between a fluorine end member, $Al_2SiO_4F_2$ (fluor-topaz) and a hypothetical hydroxyl end member, $Al_2SiO_4(OH)_2$, with the empirical formula $(Al_2SiO_4(OH,F)_2)$ [2–5]. Topaz crystallizes in the orthorhombic system, reported for crystalline materials within space group No. 62, more specifically, to the group Pbnm (62) [6]. It has a hardness of 8 in the Mohs scale and is highly resistant to a number of chemicals including hydrofluoric acid [7]. Its reported luminescent properties and effective atomic number similar to that of human tissue, makes of topaz a potential material for the field of dosimetry [4,7–10]. And although the past and recent literatures have informed on the thermoluminescent properties of natural topaz (mineral and synthetic) [11–18], thus far, no studies have reported its RL properties.

Owing to variations in composition when mined in different locations, the presence of impurities in topaz will influence its response when exposed to different radiation conditions [19]. It is thus reasonable to think that synthesized topaz would help exploiting its full potential in its response to radiation. Recently, authors synthesized topaz $(Al_2SiO_4(OH,F)_2)$ by CVD and reported its structural characteristics, formation pathway and optimum processing conditions [5].

Although several routes have been put forward for synthesizing topaz, most of them turn out to be unattractive from the economic and technological standpoints [20–24]. Owing to the relatively low processing times, pressures and temperatures, chemical vapor deposition (CVD) is an attractive alternative route for synthesis of topaz. Several precursors have been used in the synthesis of a variety of phases by CVD [25]. Sodium hexafluorosilicate (Na_2SiF_6) has been successfully used as a precursor in different investigations due to its relatively low decomposition temperature, good stability at

* Corresponding author.
E-mail addresses: evatrujillo87@gmail.com (E. Trujillo-Vázquez), martin.pech@cinvestav.edu.mx, martpech@gmail.com (M.I. Pech-Canul), jmarcass@exa.unicen.edu.ar (J. Marcazzó).

http://dx.doi.org/10.1016/j.jallcom.2017.01.159
0925-8388/

atmospheric pressure and at room temperature [26,27]. This precursor can be dissociated thermally at low temperature (≈550 °C) to generate SiF_4 (g) (according to reaction 1), which can subsequently react with the compact reactant used. In addition to SiF_4, sodium fluoride (NaF) is obtained as solid by-product but it does not participate in the reactions because it is left behind as an ash.

$$Na_2SiF_6(s) \rightarrow 2NaF(s) + SiF_4\,(g) \quad (1)$$

The aim of this work is to study the effect of compact reactant (aluminum oxide (Al_2O_3), aluminum hydroxide ($Al(OH)_3$) or kaolinite ($Al_2Si_2O_5(OH_4)$) and processing conditions by chemical vapor deposition (CVD) on topaz formation and its RL response, using sodium hexafluorosilicate as solid precursor. In addition, establish the processing conditions (temperature, time, atmosphere, and incidence angle) as well as aluminum compound compact reactant that promotes the best RL response.

2. Experimental procedure

The present investigation was carried out in two stages. In the first step, topaz was synthesized by CVD. In the second stage, the specimens were characterized by radioluminescence. The samples were prepared using aluminum oxide (A series), aluminum hydroxide (H series) or kaolinite (K series) as compact reactants and sodium hexafluorosilicate (Na_2SiF_6) as a solid precursor. The Na_2SiF_6 and the compact reactants were prepared weighing 10 g of each reagent powder and adding approximately 0.2 ml of distilled water, followed by a careful and thorough mixture with a mortar and pestle, separately. Using a uniaxial Carver press model 4350L, the Na_2SiF_6 and reactant powders were then pressed at 40 and 20 bar, respectively. Synthesis trials were conducted in three replications according to an L8 Taguchi standard experimental design. The synthesis tests were carried out in a reactor consisting of a Thermolyne tubular furnace, model 59300, provided with a 304-type stainless steel tube (the chamber) of 3.8 cm in diameter x 76.2 cm long. The Na_2SiF_6 and compacts (aluminum hydroxide, aluminum oxide or kaolinite) were positioned in the reactor, as shown schematically in Fig. 1. Table 1 shows the sample code and the experimental conditions used in the study. The tests were conducted with and without a flow of high purity nitrogen during the dwell and cooling stages (flow rate of 5 cm^3/min), at 700 and 750 °C, for 60 and 90 min. Nitrogen is used to displace the oxygen present initially in the reactor chamber and avoid formation of $Al_2SiO_4(OH)_2$, serve as gas carrier and to direct SiF_4(g) towards the reactant compact within the reactor.

Furthermore, the position of the compact reactants – Al_2O_3, Al $(OH)_3$ or $Al_2Si_2O_5(OH)_4$ –, the so called incidence angle henceforth, was varied with respect to the gas flow direction at 0 and 90°. The CVD reactor presents thermal gradients along the longitudinal axis of the tube. Based on the measured temperature profiles, the experimental temperature levels used – close to the tube ends –, were 700 and 750 °C.

After the synthesis of topaz, samples were ground in an agate mortar and sieved to-100 mesh for characterization.

The percent contribution of the abovementioned processing parameters to the variability in the amount of topaz synthesized was determined using analysis of variance (ANOVA).

In order to identify the formed phases, specimens were characterized by XRD using a diffractometer Philips model 3040 under the following conditions: excitation voltage of the anode 40 kV and current of 30 mA: monochromatic Cu K_α radiation ($\lambda = 1.5418$ E); 2θ range of 10–80°, at a scanning speed of 0.02°/s. The samples were characterized by FTIR spectroscopy using an equipment NICOLET model Avatar 320. The measurements were carried out between 4000 and 400 cm^{-1}, using KBr pellets. Morphology, distribution and composition of the samples were analyzed by SEM and energy dispersive X-ray spectroscopy (EDS) using a scanning electron microscope Philips XL30 ESEM provided with an EDX microanalysis device. Both, secondary and backscattered electron modes were used in the analysis, at an acceleration voltage between 20 and 30 kV.

The enthalpy change and Gibbs free energy change of proposed reactions for topaz formation with each of the compact reactants (A, H and K) were computed using the FactSage™ program and databases.

In the second stage of the investigation, the samples were weighed and subsequently the RL measurements were performed. RL curves were recorded at room temperature and as function of time during beta-particle irradiation with a 3.7×10^8 Bq ophthalmic ^{90}Sr beta-source placed 1 cm away from the samples. The ^{90}Sr source rendered a dose rate of 0.022 Gy/min at the sample position. The emitted light was collected by means of a $\phi = 1$ mm communication grade optical fiber (PMMA – polymethyl methacrylate) and projected onto a Sens-Tech P25PC-02 photon counting tube having sensitivity between 180 and 630 nm [28].

3. Results and discussion

The XRD patterns of A8, H8 and K8 specimens after processing by CVD can be observed in Fig. 2, allowing the identification of the reflections pertaining to AlF_3 (symbol ●) (ICDD01-080-1007), $Al_2F_{1.44}(OH)_{0.56}SiO_4$ (symbol ◊)(ICDD 01-076-0480) and Al_2O_3 (symbol □)(ICDD 00-043-1484) and $Al_2F_2(SiO_4)$ (symbol ◆)(ICDD

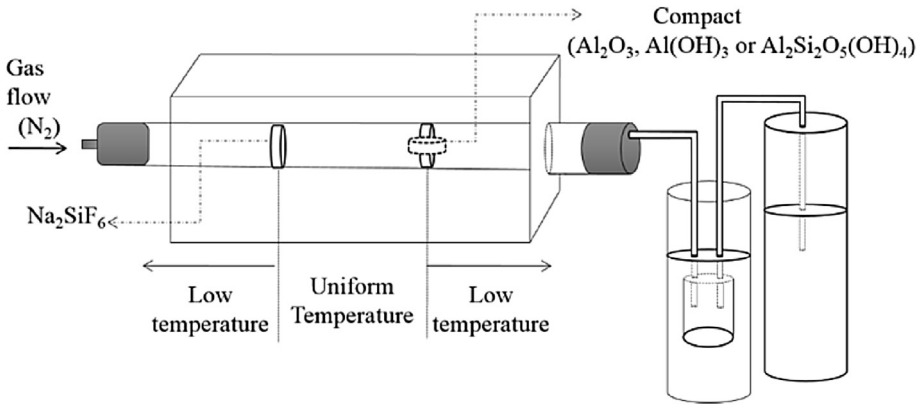

Fig. 1. Schematic diagram of the tubular reactor with solid precursor of Na_2SiF_6 and reactant compact (aluminum hydroxide, aluminum oxide or kaolinite).

Table 1
L8 Taguchi standard experimental design for synthesis of topaz by CVD.

Sample code	Temperature (°C)	Time (min)	Incidence angle (°)	Atmosphere (Nitrogen)
A1/H1/K1	700	60	90	With gas
A2/H2/K2	700	60	0	Without gas
A3/H3/K3	700	90	90	Without gas
A4/H4/K4	700	90	0	With gas
A5/H5/K5	750	60	90	Without gas
A6/H6/K6	750	60	0	With gas
A7/H7/K7	750	90	90	With gas
A8/H8/K8	750	90	0	Without gas

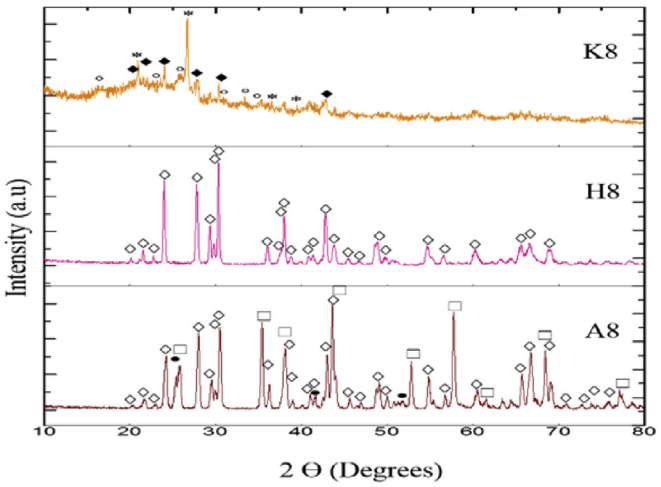

Fig. 2. Representative XRD patterns showing the presence of topaz after processing by CVD.

01-087-0576), SiO_2(symbol *)(JCPDS No. 33–1161) and $Al_{4.52}Si_{1.48}O_{9.74}$(symbol ○) (JCPDS No. 79–1457). It can be seen that topaz is formed in the three selected samples.

The infrared spectra of samples K8, H8 and A8 are shown in Fig. 3. The Stretching mode of OH^- ions is expected in the region of 3100–3600 cm^{-1}; in the same region can be seen the stretching mode H_2O, distinguishing its presence with a mode of flexion at 1600 cm^{-1}, these samples do not show this mode. In the region of 800–1050 cm^{-1} it can be observed the mode of SiO.

Representative micrographs of the microstructure of some of the studied samples, namely, K1, K8, H1, H8, A1 and A8 after

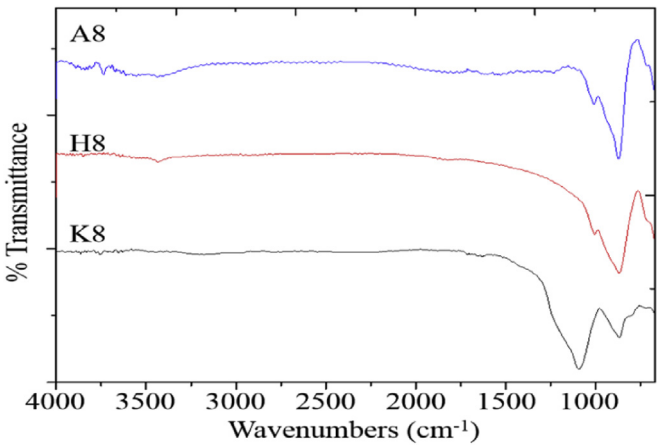

Fig. 3. FTIR spectra corresponding to samples K8, H8 and A8.

synthesis by CVD are shown in Fig. 4.

Typical SEM micrographs of samples processed from kaolinite, presented in Fig. 4 (K1 and K8), show topaz with acicular morphology. In the micrographs H1 and H8 (samples processed from aluminum hydroxide) topaz compacts constituted by cross-needle shape phases can be observed. Fibers and rectangular bars in shape of dandelions can be seen in the micrographs A1 and A8 for alumina derived samples.

Topaz synthesis from aluminum oxide can be explained in terms of endothermic and thermodynamically feasible reactions (2) and (4). In equation (2), a direct reaction occurs between Al_2O_3, the gaseous dissociation product (SiF_4) of the solid precursor (Na_2SiF_6) and the water vapor used in the compact preparation or contained as impurity in the flowing gas. Traces between 5 and 10 ppm H_2O are usually present in high purity nitrogen. In the case of reaction (4), formation of intermediate reaction products (AlF_3 and SiO_2) via reaction (3) is necessary, after which, topaz synthesis occurs by the reaction of such intermediate products with water [29].

$$Al_2O_3\,(s) + SiF_4\,(g) + H_2O\,(g) \rightarrow Al_2SiO_4F_2\,(s) + 2\,HF(g) \quad (2)$$

$\Delta G^\circ_{700} = -29.53$ kJ/mol	$\Delta G^\circ_{750} = -26.71$ kJ/mol
$\Delta H^\circ_{700} = -84.62$ kJ/mol	$\Delta H^\circ_{750} = -84.23$ kJ/mol

$$Al_2O_3\,(s) + 1.5\,SiF_4\,(g) \rightarrow 2AlF_3(s) + 1.5\,SiO_2\,(s) \quad (3)$$

$\Delta G^\circ_{700} = -40.65$ kJ/mol	$\Delta G^\circ_{750} = -32.06$ kJ/mol
$\Delta H^\circ_{700} = -210.3$ kJ/mol	$\Delta H^\circ_{750} = -204.96$ kJ/mol

$$2AlF_3\,(s) + SiO_2\,(s) + 4H_2O\,(g) \rightarrow Al_2SiO_4\,(F, OH)_2\,(s) + 4\,HF\,(g) + H_2\,(g) \quad (4)$$

Reactions 5 and 7 are two proposed routes for topaz synthesis starting from aluminum hydroxide. In the former, topaz is produced by the direct reaction between aluminum hydroxide and silicon tetrafluoride, whilst in the latter it is formed indirectly by the occurrence of intermediate reaction products (aluminum fluoride and silicon dioxide) via reaction (6), which subsequently react with aluminum hydroxide (reaction 7).

$$2\,Al(OH)_3\,(s) + SiF_4\,(g) \rightarrow Al_2SiO_4F_2\,(s) + 2H_2O\,(g) + 2\,HF\,(g) \quad (5)$$

$\Delta G^\circ_{700} = -299$ kJ/mol	$\Delta G^\circ_{750} = -315.7$ kJ/mol
$\Delta H^\circ_{700} = 26.81$ kJ/mol	$\Delta H^\circ_{750} = 21.91$ kJ/mol

$$Al(OH)_3\,(s) + 1.5\,SiF_4\,(g) \rightarrow AlF_3\,(s) + 1.5\,SiO_2(g) + 3\,HF(g) \quad (6)$$

$\Delta G^\circ_{700} = -149$ kJ/mol	$\Delta G^\circ_{750} = -159.7$ kJ/mol
$\Delta H^\circ_{700} = 56.7$ kJ/mol	$\Delta H^\circ_{750} = 58.9$ kJ/mol

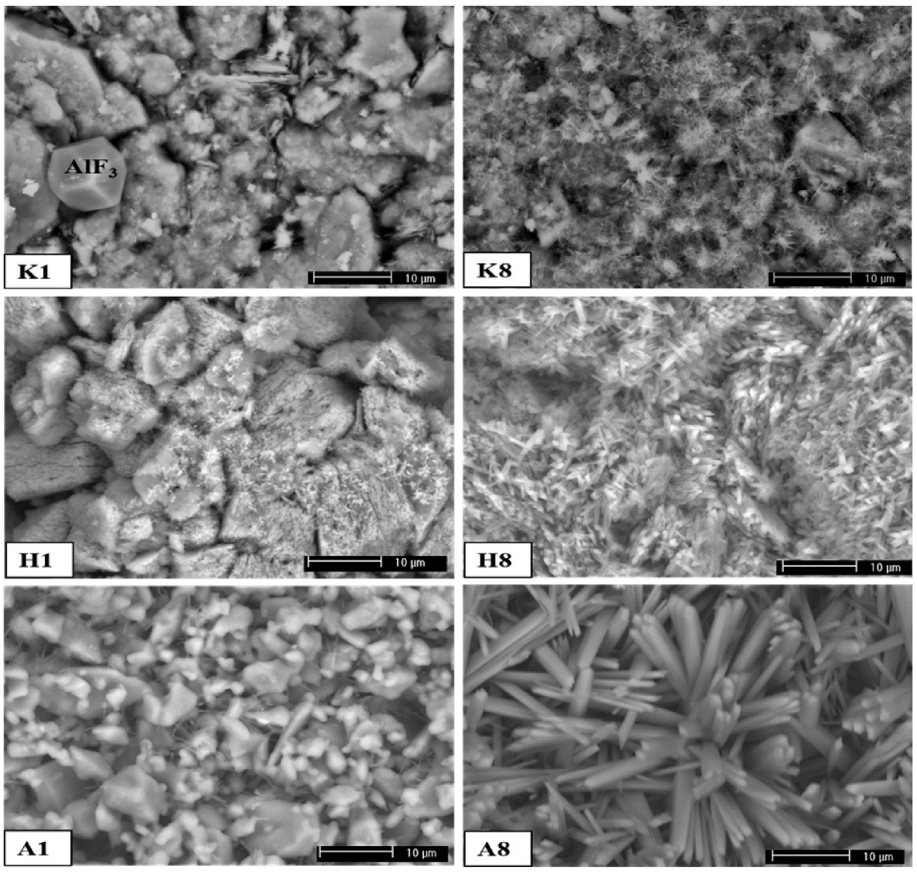

Fig. 4. Representative SEM micrographs of specimens K1, K8, H1, H8, A1 and A8 after synthesis trials.

$$4\ Al(OH)_3\ (s) + 2\ AlF_3\ (s) + 3\ SiO_2\ (s) \rightarrow 3Al_2SiO_4F_2\ (s) + 6H_2O\ (g) \quad (7)$$

$\Delta G^\circ_{700} = -599.2$ kJ/mol	$\Delta G^\circ_{750} = -627$ kJ/mol
$\Delta H^\circ_{700} = -32.91$ kJ/mol	$\Delta H^\circ_{750} = -52.12$ kJ/mol

It should be noted that although the reactions of both routes are thermodynamically feasible, reaction (7) through intermediate reaction products, is however, significantly more viable thermodynamically than the direct route. Furthermore, topaz formation is more thermodynamically feasible with increase in temperature.

Formation of topaz using kaolinite as the compact reactant is explained by the exothermic and thermodynamically viable reaction with SiF_4, having silicon dioxide as a solid reaction product, according to reaction (8).

$$Al_2Si_2O_5(OH)_4\ (s) + SiF_4\ (g) \rightarrow Al_2SiO_4F_2\ (s) + 2\ HF\ (g) + 2\ SiO_2(s) + H_2O\ (g) \quad (8)$$

$\Delta G^\circ_{700} = -201.90$ kJ/mol	$\Delta G^\circ_{750} = -216.73$ kJ/mol
$\Delta H^\circ_{700} = 85.59$ kJ/mol	$\Delta H^\circ_{750} = 87.84$ kJ/mol

It should be pointed out that the gas reaction products in all experimental trials were bubbled up in a neutralizer device built-in in the experimental set-up (See Fig. 1).

Fig. 5 shows results from phase semi-quantitative analysis using the XPowder® program of topaz formed in the three types of compacts (aluminum oxide, aluminum hydroxide and kaolinite). Whilst "series H" presented the highest percentage of topaz formed, "series K" showed the lowest percentage. Although the quantification of topaz is not shown for K1 sample, due to the limitation of XRD equipment for quantifying low amounts of phases, topaz can be observed in micrograph K1 (see Fig. 4). The greater amount of topaz formed using aluminum hydroxide might be explained by its larger reaction thermodynamic feasibility, compared with those of the reactions involving aluminum oxide and kaolinite.

Results from the analysis of variance (ANOVA) presented in Table 2 show that the parameter that most significantly influences the variability in the amount of topaz in compact reactants of kaolinite, aluminum hydroxide and aluminum oxide is temperature with contributions of 99, 31 and 78%, respectively. By contrast, the parameters that have low contributions to the variability in the formation of topaz from the compact reactants are atmosphere and incidence angle. The low contribution of the atmosphere could be related to the fact that the gas feed is important only in the heating stage, when decomposition of the solid precursor starts. The low P values of incidence angle in the three cases indicate that regardless of sample angle position, the variability in the amount of topaz formed is insignificant. It is likely that under the used experimental conditions, saturation of the reactor chamber with SiF_4 gas species significantly downgrades the effect of sample angle position on the amount of topaz formed.

RL spectra emission of H8, A8 and K8 samples are presented in Fig. 6. These samples were selected because they showed the highest amounts of topaz formation for each series. As it can be seen from the figure, the spectra have a broad emission band

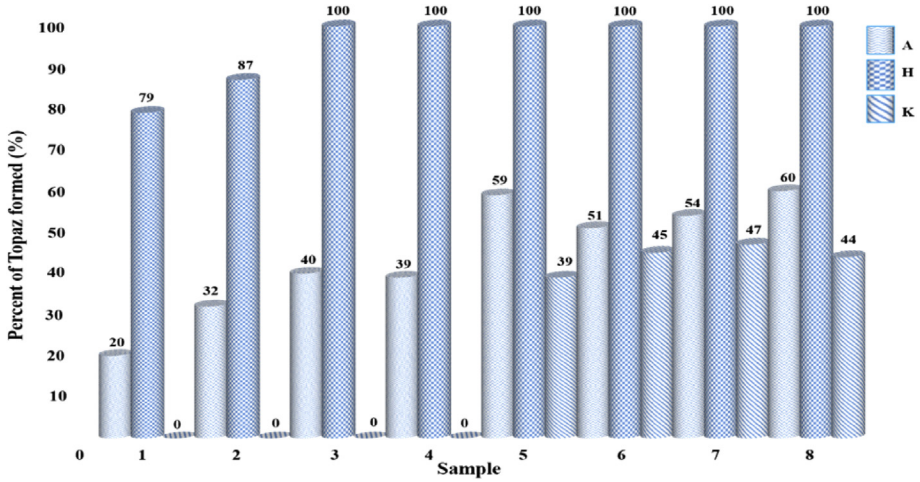

Fig. 5. Percent of topaz formed in compacts of aluminum oxide (A), aluminum hydroxide (H) and kaolinite (K).

Table 2
Pooled ANOVA table for the percentage of topaz formed.

Factor	SS			V			P (%)		
	K	H	A	K	H	A	K	H	A
Angle position (P)	1	6.8	10	1	6.8	10	0	2	1
Temperature (T)	3828	139.4	1081	3828	139.4	1081	99	31	78
Angle position x temperature (P X T)	_	6.8	_	_	6.8	_	_	2	_
Atmosphere (A)	10	6.8	91	10	6.8	91	0	2	7
Angle position x atmosphere (P X A)	_	139.4	_	_	139.4	_	_	31	_
Time (t)	6	6.8	120	6	6.8	120	0	31	9
Error	18	6.8	88	18	6.8	88	1	1	5
Total	3863	445.72	1390	3863	445.72	1390	100	100	100

SS is sum of squares, V is variance, and P is percentage contribution.

centered at 390 nm, attributed to $(H_3O_4)^0$ center emitting at 380 nm [2].

Two color centers – $(AlO_4)^0$ and $(H_3O_4)^0$ – typically observed in quartz and emitting at 460 and 380 nm, respectively, have been reported for topaz by Souza et al. [2]. Moreover, studies conducted by McKeever et al. reported the formation of $(AlO_4)^0$ color centers and their contribution to TL response. Furthermore, Nuttall and Weil focused their attention on the $(H_3O_4)^0$ center [30]. It was further determined that both centers are similar, except for the fact that in the latter, three protons occupy the Si^{4+} site instead of the Al^{3+} ion in the former [31].

Besides, it is evident from Fig. 6 that the RL emission (defined as the area under the RL curve) of H8 sample is more than two and five times greater than RL emission of A8 and K8 samples, respectively. In order to determine the best processing conditions (temperature, time, atmosphere and incidence angle), the results of the RL intensity of the highest RL response series, namely, samples H1–H8, are shown in Fig. 7. Although all the synthesized specimens (H series) showed RL response, samples H3 (processed at 700 °C, 90 min, 90° $Al(OH)_3$ of incidence angle and without gas) and H4 (processed at 700 °C, 90 min, 0°, and with gas) exhibited the highest intensity, which could be related to the amount of topaz formed (100%) and to the presence of defects.

Dantas et al. [32] showed a comparison of the photostimulated emission of topaz and quartz and found that the emission bands are similar for both the topaz and quartz samples. They attributed this similarity to the fact that in silicates, the luminescence centers are $(AlO_4)^0$ and $(H_3O_4)^0$. These centers are formed by the ion substitution of Si^{4+} by Al^{3+} or $3H^+$. In the same work, it is remarked that Souza et al. [33] and Ribbe and Gibbs [34] observed previously that

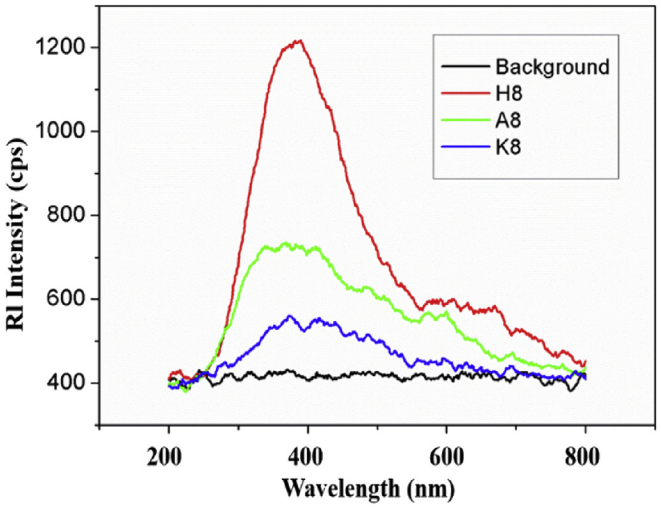

Fig. 6. Radioluminescence spectra of specimens H8, A8 and K8.

the wavelength range of the TL emission of this mineral is similar to those of the silicates.

It is worth mentioning that no changes in RL sensitivity during irradiation are observable from these samples. This behavior could be related either with a rapid equilibrium attainment between charges trapping and detrapping rates during irradiation or with a low concentration of shallow traps [35]. Furthermore, it is possible to observe a small signal of phosphorescence, i.e. afterglow, in the

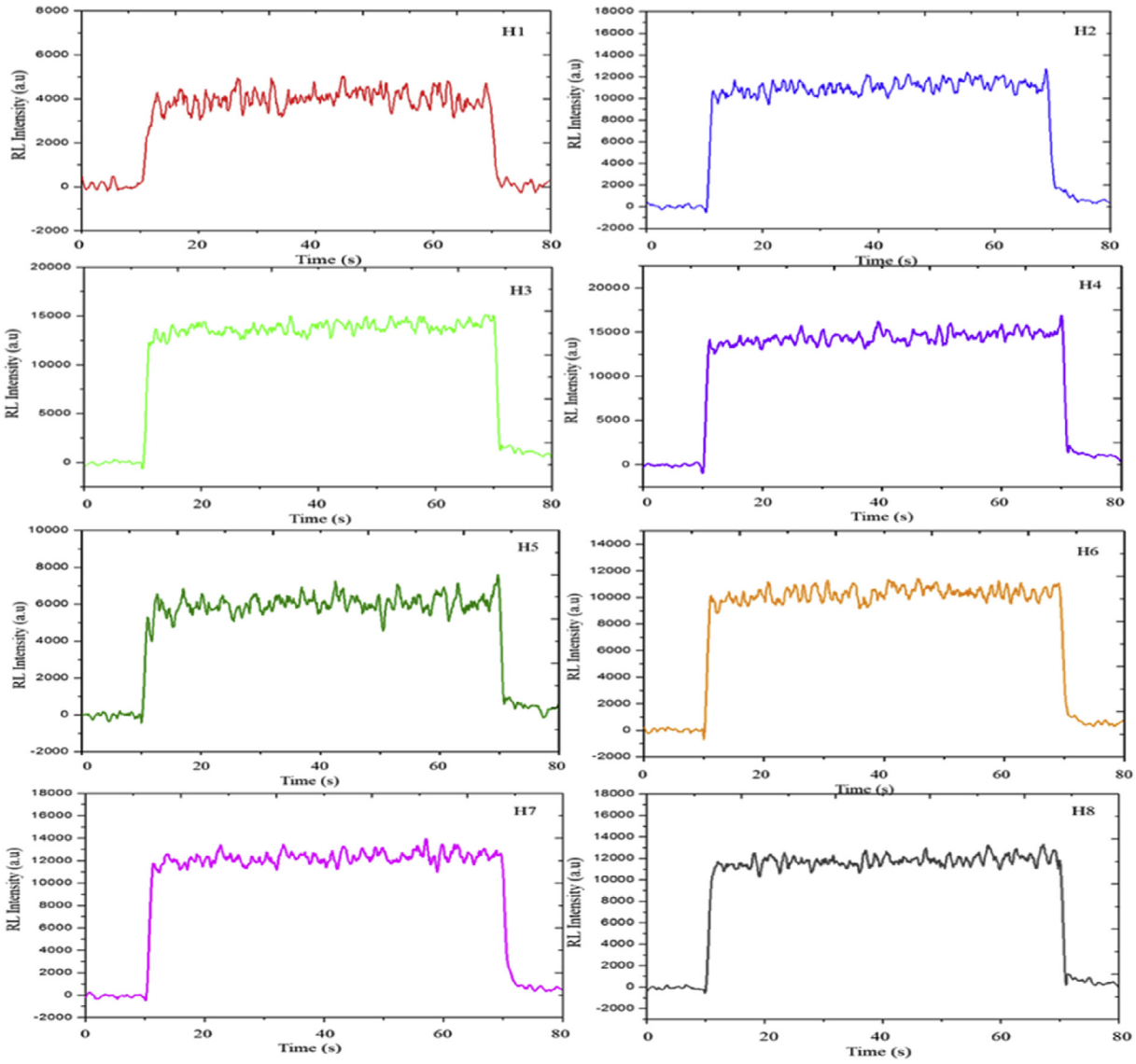

Fig. 7. RL response graphs of H series samples irradiated with ^{90}Sr.

first 5 s after irradiation and then, disappears completely. It represents an advantage over other scintillators as the C-doped aluminum oxide, whose afterglow could be still important after several minutes following irradiation [35,36].

In the current study it was found that topaz formed using aluminum hydroxide showed the maximum RL response whilst samples processed from aluminum oxide and kaolinite exhibit responses two and five times lesser than the first one. Nonetheless, topaz prepared from aluminum oxide in a previous work by the same research group, exhibited exceptional TL properties [17].

The reason behind the RL behavior in samples prepared from aluminum hydroxide could be related to the concentration of color centers. Specifically, the RL emission is attributed to the existence of the center $(H_3O_4)^0$, because as it can be observed in the spectrum (Fig. 6), a broad emission band is centered at 390 nm. And because of its proximity, this center is assumed in the current work, to be the one reported at 380 nm.

Additional measurements performed in samples (H1–H8) treated thermally at 500 °C, showed that none of them exhibited RL response. A study by Kristianpoller et al. reported that the center $(H_3O_4)^0$ decays significantly over the temperature range from room temperature to 150 °C [31,37]. Hence, the lack of RL behavior after the thermal treatments and the RL response of the samples (H1–H8) in the untreated condition, substantiate the postulate that the center $(H_3O_4)^0$ is responsible of the radioluminescent emission in samples prepared using aluminum hydroxide. Moreover, since this center may be related to hydrogen [31,38], it is expected that this element occurs in higher concentration when aluminum hydroxide compact reactant is used in the synthesis.

4. Conclusions

For the first time the radioluminescence properties of topaz synthesized by chemical vapor deposition (CVD) using Na_2SiF_6 as silicon solid precursor and three different compact reactants – namely, aluminum oxide (A), aluminum hydroxide (H) and kaolinite (K) – have been investigated. It was found that topaz is formed in a variety of morphologies (fibers, rectangular bars and compact phases presenting cross-needle shape) using the three reactants, though in different amounts of 60%, 100% and 47%,

respectively. A series of reaction pathways is proposed for topaz formation using the three compact reactants. By use of aluminum oxide and aluminum hydroxide, two reaction pathways for each, i.e., directly and indirectly through the formation of intermediate reaction products are put forward. Only topaz samples synthesized using aluminum hydroxide exhibited RL response. Even more, the samples identified as H3 and H4, processed at 700 °C for 90 min, showed the best RL emission. The RL response in (H)-derived samples is explained by the existence of $(H_3O_4)^0$ color centers, emitting at 390 nm. This color center is related to the presence of hydrogen, which is more likely present in samples prepared from aluminum hydroxide than in samples processed from (A) and (K) compact reactants. The attribution of the $(H_3O_4)^0$ color centers to the RL behavior is corroborated by treating thermally the samples at 500 °C, after which no RL emission was observed. The RL response and effective atomic number of topaz similar to that of human tissue suggest its potential applications in dosimetry.

Acknowledgements

Ms. E. Trujillo-Vázquez gratefully acknowledges Conacyt (National Council of Science and Technology) for granting a Doctoral scholarship. Also, thanks to “Instituto de Física Arroyo Seco (UNCPBA)” for the facilities provided for her academic stay. Authors are also grateful to Mr. Sergio Rodríguez-Arias his support in the characterization by XRD. Dr. Marcazzó acknowledges the financial support received from PICT 2015–2647 (ANPCyT, Argentina) and PIP 800/2015 (CONICET, Argentina).

References

[1] Axel Ritter, Smart Materials in Architecture, Interior Architecture and Design, Springer Science & Business Media, Bad Nevenahr- Ahrweiler, 2006. USA.
[2] Divanizia N. Souza, José Fernandes de Lima, Mário Ernesto G. Valerio, Cristiano Fantini, Marcos A. Pimenta, Roberto L. Moreira, Linda V.E. Caldas, Influence of thermal treatment on the Raman, infrared and TL responses of natural topaz, Nucl. Instr. Meth.in Phys. Res. B 191 (2002) 230–235.
[3] M.D. Barton, H.T. Haselton Jr., B.S. Hemingway, O.J. Kleppa, R.A. Robie, The thermodynamic properties of fluor-topaz, Am. Min. 67 (1982) 350–355.
[4] C. Marques, A. Falcão, R.C. da Silva, E. Alves, Structural and optical characterization of topaz implented with Fe and Co, Nucl. Instr. Meth.in Phys. Res. B 191 (2002) 312–316.
[5] E. Trujillo-Vázquez, M.I. Pech-Canul, Formation pathway, structural characterization and optimum processing parameters of synthetic topaz-$Al_2SiO_4(OH,F)_2$-by CVD, J. Solid State Chem. 230 (2015) 350–356.
[6] T. Hahn, International Tables for Crystallography, Volume A: Space-group Symmetry, fifth ed., Springer, Norwell, MA, USA, 2005, pp. 298–299.
[7] P.L. Bocko, D.H. Crooker, L.M. Echeverria, Method for Synthesizing Topaz, US Patent No. 4940477A, USA, 1990.
[8] M. Akizuki, M.S. Hampar, J. Zussman, An explanation of anomalous optical properties of topaz, Mineral. Mag. 43 (1979) 237–241.
[9] M.E. Medhat, Study of the mass attenuation coefficients and effective atomic numbers in some gemstones, J. Radioanal. Nucl. Chem. 293 (2012) 555–564.
[10] K. Mahesh, Pao-shan Weng, C. Furetta, Thermoluminescence in Solids and its Applications, Nuclear Technology Publishing, Ashford, England, 1989.
[11] A.L. Moss, J.W. McKleen, Thermoluminescent properties of topaz, Health Phys. 34 (1978) 137–140.
[12] J. Azorin Nieto, Termoluminiscencia del SiO_2, del $Al_2(F,OH)_2SiO_4$ y del $Na_2OAl_2O_36SiO_2$ para la dosimetría de la radiación ionizante, UNAM, México, 1979. Master's thesis.
[13] C.A. Ferreira Lima, L.A.R. Rosa, P.G. Cunha, The thermoluminescent properties of Brazilian topaz, Appl. Radiat. Isot. 37 (1986) 135–137.
[14] D.N. Souza, J.F. de Lima, M.E.G. Valerio, Thermoluminescence of natural topaz crystals of differing genesis, Mater. Sci. Forum 239–241 (1997) 765–768.
[15] E.G. Yukihara, E. Okuno, On the thermoluminescent properties and behavior of brazilian topaz, Nucl. Instr. Meth.in Phys. Res. B 141 (1998) 514–517.
[16] D.N. Souza, J.F. de Lima, M.E.G. Valerio, L.V.E. Caldas, Thermally stimulated luminescence and EPR studies on topaz, Appl. Radiat. Isot. 64 (2006) 906–909.
[17] E. Trujillo-Vázquez, M.I. Pech-Canul, J. Marcazzó, Thermoluminescent characterization of Al_2O_3 – derived synthetic topaz, J. Alloy Compd. 689 (2016) 500–506.
[18] V. Correcher, J. Garcia-Guinea, C. Martin-Fernandez, N. Can, Thermal effect on the cathode and thermoluminescence emission of natural topaz (Al_2SiO_4(-F,OH)$_2$, CORALS-2011 CONFERENCE on the Micro-Raman and luminescence in Earth and Space Sciences, España (2011) p.p 20.
[19] C.M.S. de Magalhaes, Z.S. Macedo, M.E.G. Valerio, A.C. Hernandes, D.N. Souza, Preparation of composites of topaz enbedded in glass matrix for applications in solid state thermoluminescence dosimetry, Nucl. Instr. Meth.in Phys. Res. B 218 (2004) 277–282.
[20] P.E. Rosenberg, Compositional variations in synthetic topaz, Am. Mineral. 57 (1972) 169–187.
[21] A.M. Abdel Rehim, Thermal and XRD analysis of synthesis of fluoro-topaz, Thermochim. Acta 538 (2012) 29–35.
[22] W.A. Deer, R.A. Howie, J. Zussman, Rock Forming Minerals, 1A, Orthosilicates, second ed., The Geological Society, United Kingdom, 1971.
[23] S. Somiya, S.I. Hirano, M. Yoshimura, H. Shima, Hydrothermal synthesis of topaz crystals, Hydrothermal React. Mater. Sci. Eng. 5 (1989) 271–279.
[24] W.A. Deer, R.A. Howie, J. Zussman, Rock Forming Minerals, 5A, Non Silicates Oxides, Hydroxides and Sulphides, second ed., The Geological Society, United Kingdom, 2011.
[25] K.L. Choy, Chemical vapour deposition of coatings, Prog. Mater. Sci. 48 (2003) 57–170.
[26] A.L. Leal-Cruz, M.I. Pech-Canul, Situ synthesis of Si_3N_4 from Na_2SiF_6 as a silicon solid precursor, Mater. Chem. Phys. 98 (2006) 27–33.
[27] M.I. Pech-Canul, J.L. de la Peña, A.L. Leal-Cruz, Effect of processing parameters on the deposition rate of Si_3N_4/Si_2N_2O by chemical vapor infiltration and the in situ thermal decomposition of Na_2SiF_6, Appl. Phys. A 89 (2007) 729–735.
[28] M. Santiago, J. Marcazzó, C. Grasselli, A. Lavat, P. Molina, F. Spano, E. Caselli, Thermo- and radioluminescence of undoped and Dy-doped strontium borates prepared by sol-gel method, Radiat. Meas. 46 (2011) 1488–1491.
[29] A.M. Abdel Rehim, Application of thermal analysis to mineral synthesis, J. Therm. Anal. 48 (1997) 177–202.
[30] R.H.D. Nuttall, J.A. Weil, Two hydrogenic trapped-hole species in α- Quartz, Solid State Commun. 33 (1980) 99–102.
[31] X.H. Yang, S.W. McKeever, The pre-dose effect in crystalline quartz, J. Phys. D. Appl. Phys. 23 (1990) 237–244.
[32] S.C. Dantas, M.E. Giroldo Valerio, M.A. Couto dos Santos, D.N. Souza, Photo-induced emission and thermoluminescence in topaz, Nucl. Instr. Meth.in Phys. Res. B 250 (2006) 386–389.
[33] D.N. Souza, J.F. Lima, M.E.G. Valerio, J.M. Sasaki, L.V.E. Caldas, Radiation-induced charge trapping and recombination process in natural topaz studied by TL, EPR and XRD, Nucl. Instr. Meth.in Phys. Res. B 218 (2004) 123–127.
[34] P.H. Ribbe, G.V. Gibbs, The crystal structure of topaz and its relation to physical properties, Am. Mineral. 56 (1971) 24–30.
[35] S.M.S. Damkjaer, C.E. Andersen, M.C. Aznar, Improved real-time dosimetry using the radioluminescence signal from Al_2O_3:C, Radiat. Meas. 43 (2008) 893–897.
[36] P. Molina, M. Santiago, J. Marcazzó, F. Spano, N. Khaidukov, E. Caselli, Radio-luminescence of rare-earth doped potassium yttrium fluorides crystals, Radiat. Meas. 46 (2011) 1361–1364.
[37] N. Kristianpoller, R. Chen, M. Israeli, Dose dependence of thermoluminescence peaks, J. Phys. D. Appl. Phys. 7 (1974) 1063–1072.
[38] X.H. Yang, S.W. McKeever, The pre-dose effect in crystalline quartz, J. Phys. D. Appl. Phys. 23 (1990) 237–244.